Proceedings World Geothermal Congress 2005
Antalya, Turkey, 24-29 April 2005

Analysis and Interpretation of Naphthalene Disulfonate Tracer Tests at the Mahanagdong Geothermal Field, Philippines

P. O. Molina, T. Tanaka, R. Itoi, F. L. Siega and M. S. Ogena

Department of Earth Resources Engineering, Graduate School of Engineering, Kyushu University, 6-10-1 Hakozaki, Higashi-ku, Fukuoka, Japan 812-0053

molina@mine.kyushu-u.ac.jp

Keywords: tracer, naphthalene disulfonate, Mahanagdong

ABSTRACT

To define the hydrological flow paths and rate of return/inflow of cooler peripheral waters in the Mahanagdong geothermal reservoir, three types of naphthalene disulfonate (NDS) tracers were introduced in three different wells in January 2003. 1,6-NDS was injected in Well MG-4DA to trace the movement of the Paril groundwater. 1,5-NDS and 2,6-NDS were injected in Wells MG-21D and MG-5RD, respectively, to characterize the power plant condensates and separated brine injected at the MGB3 and MGRD1 injection pads. Of the twenty wells monitored for more than nine months, twelve wells showed positive tracer responses from one or two of the three injection wells, indicating the influence of several types of peripheral waters. The tracer test data was analyzed using a multi-path model based on the one-dimensional transport equation for porous media. The principal outputs from the analysis were recovery and discharge fractions and average residence time of the fluids. Analysis results established the hydrological connection between the injection and production wells, quantified the effect of returns in terms of mass fractions, and estimated the velocity of return/inflow. A discussion of the results is presented.

1. INTRODUCTION

The Mahanagdong geothermal field is a part of a large geothermal reservation in the island of Leyte in the Philippines. This geothermal reservation, termed as the Greater Tongonan Geothermal Field (GTGF), has been explored and operated by the PNOC Energy Development Corporation (PNOC-EDC) since the late 1970s. The Mahanagdong field lies in the southern part of the GTGF, separated from the northern field by a cold and impermeable barrier. It is about 8 km^2 and is currently producing about 176 MWe.

The Mahanagdong field, comprised of 3x60 MWe condensing turbine main plants with an additional 3x6.4 MWe non-condensing backpressure turbine optimization plants, is divided into two sectors – Mahanagdong-A and Mahanagdong-B – separated by a topographic low related to the Mamban fault (Fig. 1). Mahanagdong-A, which is made up of a 2x60 MWe main plant and a 2x6.4 MWe optimization plant, has a steam requirement of about 250 kg/s. It taps into a dominantly hot area with neutral pH fluids in the southern part of the field through 13 production wells. Mahanagdong-B faced serious constraints meeting the steam requirement of about 130 kg/s. The northern part of the field comprises of acidic fluids in the north, cooler waters in the west, and high-gas fluids in the east, leaving a limited area in the central part where 6 production wells tap the reservoir.

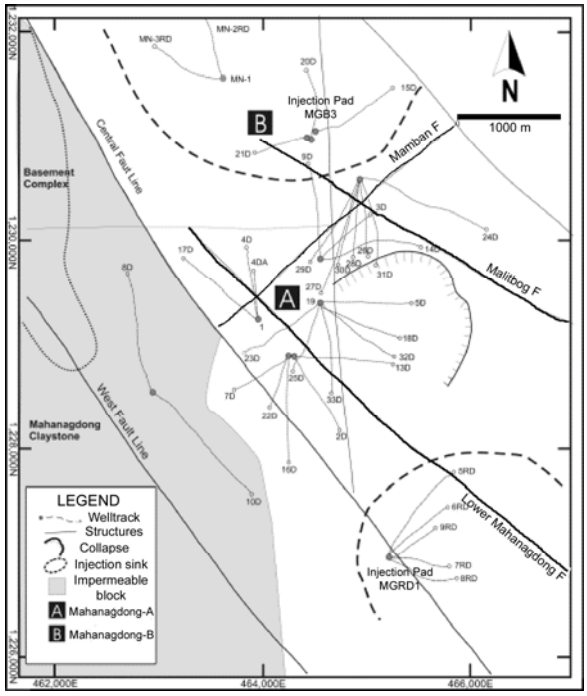

Figure 1. Location map of the Mahanagdong geothermal field

The main plants commenced commercial operation in July 1997 while the optimization plants were commissioned later the same year. The optimization or topping cycle plants (TCP) utilize high-pressure (~1.2 MPa) separated steam from the production wells. The discharges from these plants are then fed to the main plants with the steam from the flashed brine (second separation at 0.7 MPa) obtained after the initial high-pressure separation.

The first few years of commercial exploitation of the Mahanagdong reservoir illustrated a level of production that exceeded the sustainable level, that is, the system could not cope with the steam demand. Commercial exploitation brought about rapid reservoir changes, some of which proved detrimental to the steam supply.

Various steps have been taken to relieve the system of the stresses brought by the commercial operations. One of the steps implemented is waste injection management by prioritizing the injection wells located farthest from the production sectors. To aid injection management, several kinds of tracers have been used to understand the invasion of cooler fluids into the production sectors.

2. THE TRACER TEST USING NAPHTHALENE DISULFONATE (NDS)

This tracer test was conducted to define the hydrological flow paths and rate of return/inflow of cooler peripheral waters in the Mahanagdong field considering the extent of pressure drawdown after 5 years of commercial exploitation. These waters include the Paril groundwater, power plant condensates, and separated brine injected at pads MGB3 and MGRD1 (Fig.1).

Three types of naphthalene disulfonate (NDS) tracers were used in this test: 1,5-NDS, 1,6-NDS and 2,6-NDS. These are part of the 7 naphthalene sulfonates that have been tested in the laboratory and in the field for use as geothermal tracers.

The three types of tracers were injected separately at three injection points as indicated in Fig. 2. Well MG-5RD is one of the injection wells located at pad MGRD1 utilized for the disposal of brine from Mahanagdong-A. Well MG-21D is one of the acid wells drilled in the northern section of the field. It was converted to an injection well for Mahanagdong-B. Well MG-4DA was drilled as a production well but due to a substantial influx of cooler water from the Paril area, its fluid temperature was decreased to 170°C. Thus it was deemed unfit for production and is now utilized to trace the flow of the Paril groundwater.

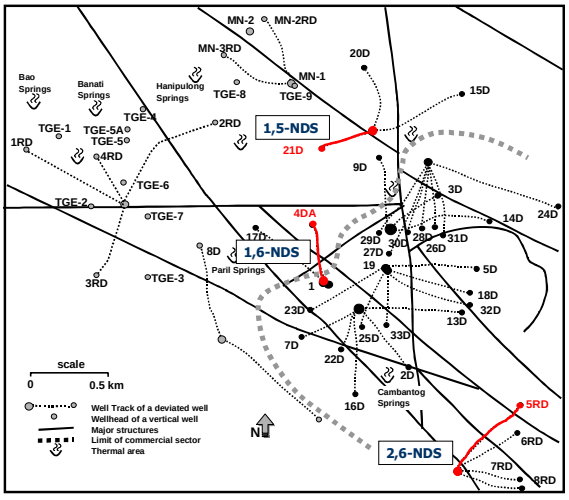

Figure 2. Map of the Mahanagdong field indicating the type of NDS tracer injected in three different locations

The injection of NDS tracers was conducted on January 13-15, 2003. Approximately 600 kg of each type of tracer in powder form was dumped into a slurry mixer and dissolved in fresh water with a dissolution ratio of 300 l water per 50 kg of tracer. The tracer slurry was then injected into the well through the wing valve using a pump. Injection was conducted in the shortest possible time to simulate an instantaneous injection in the reservoir.

Monitoring for tracer returns to the production sector was originally programmed from the day of injection to the end of September 2003. Monitoring was extended to the end of December 2003 according to the resulting breakthrough curves.

A total of twenty wells (MG-1, MG-2D, MG-3D, MG-7D, MG-13D, MG-14D, MG-16D, MG-18D, MG-19, MG-22D, MG-23D, MG-24D, MG-26D, MG-27D, MG-28D, MG-29D, MG-30D, MG-31D, MG-32D and MG-33D) were monitored for tracer returns. Water samples were collected from these wells at least twice a week.

In each of the monitored wells, the two-phase discharge line was tapped by a cooling coil. The two-phase sample was condensed and collected as pure liquid at the end of the coil.

Water samples collected from the monitor wells were scanned for the three types of tracers using high performance liquid chromatography (HPLC). HPLC allows for the separation of the polyaromatic sulfonates from each other and from interferences that occur naturally in the reservoir.

3. THEORY

The flow of a solute (tracer) between an injection point and an observation point is usually described by the well known convection-dispersion-diffusion equation in one dimension:

$$\frac{\partial C}{\partial t} = D\frac{\partial^2 C}{\partial^2 x} - u\frac{\partial C}{\partial x} \tag{1}$$

Here, C is the tracer concentration [mg/l], t is the time [h], u is the fluid velocity [m/h], x is the distance from the injection point [m], and D is the dispersion coefficient [m^2/h]. Molecular diffusion is considered negligible in this study.

Assuming instantaneous injection in the reservoir, the following formula is used to obtain the tracer concentration at the observation point:

$$C^* = \frac{1}{2}\left\{erfc\left(\frac{a-t}{2\sqrt{(a/Pe)t}}\right) + \exp(Pe)erfc\left(\frac{a+t}{2\sqrt{(a/Pe)t}}\right)\right\}$$

$$-\frac{1}{2}\left\{erfc\left(\frac{a-(t-t_1)}{2\sqrt{(a/Pe)(t-t_1)}}\right) + \exp(Pe)erfc\left(\frac{a+(t-t_1)}{2\sqrt{(a/Pe)(t-t_1)}}\right)\right\} \tag{2}$$

where C^* is the dimensionless concentration [-], a is the average residence time of fluids [h], Pe is the function mobility ratio (Peclet number) [-], and $erfc$ is the complementary error function. Furthermore,

$$C^* = \frac{C - C_0}{C_I - C_0} \tag{3}$$

$$a = x/u \tag{4}$$

and

$$Pe = ux/D \tag{5}$$

where C_0 and C_I are the background and injection concentrations [mg/l], respectively.

This study uses a multi-path model that can analyze tracer recovery curves with multiple peaks. If n is the number of paths from injection to production well, then the tracer concentration and the total recovery fraction (f) in each production fluid is calculated by

$$C_w^* = \frac{q_I v_I}{q_w v_w} \sum_{k=1}^{n} f_k C_k^* \quad (6)$$

where $\sum_{k=1}^{n} f_k \leq 1$. Here, q_I and q_w are the injection and discharge flow rates [kg/s], and v_I and v_w are the corresponding specific volumes [m^3/kg].

Analysis is performed using nonlinear least squares fitting. A minimum number of paths is assumed between the injection and production well, and the tracer recovery curve of each path is calculated on the basis of the initial estimates of the parameters *f*, *a* and *Pe*. The combined tracer recovery curve is calculated to fit the observed data by minimizing the sum of squares of the residuals (SSR) given by

$$SSR = \sum \left(C_w^* - C\right)^2 \quad (7)$$

The Akaike's Information Criterion (AIC) is used to compare the data fit with different number of paths. AIC is written as

$$AIC = m \ln(SSR) + 2M \quad (8)$$

where *m* is the number of data points and *M* is the number of independent parameters.

The principal output of the model are *f*, *a* and *Pe*. When *x* is known, then the average fluid velocity (*u*) and the dispersion coefficient (*D*) are easily obtained. In addition, the discharge fraction is given by

$$\alpha = f \frac{q_I}{q_w} \quad (9)$$

4. RESULTS AND DISCUSSION

Of the twenty wells monitored for more than nine months, only twelve wells showed positive tracer response from one or two of the injection wells, indicating the influence of several types of peripheral waters. The results of the test are summarized in Table 1.

The 1,5-NDS injected in Well MG-21D showed positive returns in five wells (MG-3D, MG-14D, MG-28D, MG-30D and MG-31D) indicating a direct hydrological connection between these well pairs. The recovery profiles (Fig. 3) show sharp breakthrough curves that indicate high velocities and low dispersion. The arrival of the tracer in Wells MG-3D (Fig. 3(a)) and MG-28D (Fig. 3(b)) were first detected a few days after injection while in Wells MG-14D (Fig. 3(c)), MG-30D (Fig. 3(d)) and MG-31D (Fig. 3(e)) detection was within the first two weeks. Figure 3 also shows the simulated recovery curves compared with the observed data. Two paths gave the best fit for Wells MG-3D, MG-14D and MG-28D. The late time data for Wells MG-30D and MG-31D may indicate a second flow channel but the number of available data points is not enough to make a good fit.

Table 2 shows the results of numerical simulation for the 1,5-NDS test. The total recovery fraction from the wells is 0.037 or about 22 kg out of the original 600 kg of tracer injected. Well MG-3D exhibits the highest recovery fraction at 0.019 while Well MG-31D exhibits the lowest at 0.003. These values translate to discharge fractions of 0.034 and 0.004, respectively, based on the injection and production rates during the test. These values also indicate that Well MG-3D is most affected by Well MG-21D among the wells with positive returns.

Table 1. Summary of NDS Tracer Test Results (O marks indicate tracer concentrations greater than 3 ppb)

	1,5-NDS (MG-21D)	1,6-NDS (MG-4DA)	2,6-NDS (MG-5RD)
MG-3D	O		
MG-14D	O		
MG-26D		O	
MG-27D		O	
MG-28D	O		
MG-29D		O	
MG-30D	O	O	
MG-31D	O	O	
MG-7D			O
MG-16D			O
MG-2D			O
MG-22D			O

Geological data indicate the Malitbog Fault (Fig. 1) as a possible conduit of fluids from Well MG-21D to Wells MG-3D, MG-14D and other MG-DL wells.

Monitoring for 1,6-NDS indicated the connection between Well MG-4DA and five production wells (MG-27D, MG-28D, MG-29D, MG-30D and MG-31D). The recovery profiles in Fig. 4 indicate a slow-moving fluid from Well MG-4DA. The tracer was first detected in Well MG-29D (Fig. 4(b)) at day 68 followed by Well MG-30D (Fig. 4(d)) at day 75. High dispersion is indicated although the profiles still show incomplete breakthrough curves at the start of September 2003 (the extent of available data).

It should be noted that the model used in this study considers an injection-production well pair with constant flow rates to calculate the best values for the parameters. However, being non-commercial, there is no known value for the injection flow rate of Well MG-4DA during the tracer test. So that the existing model may be applied, the groundwater down flow rate inside the well was used as a minimum injection rate. In addition, to calculate the fluid properties, the well temperature of 170°C was used as the maximum value. These assumptions directly affect the values used in the calculations such that the results of the simulation may only be considered, at best, rough estimates. Furthermore, some of the data in Wells MG-27D (Fig. 4(c)) and MG-31D (Fig. 4(e)) were ignored based on their semi-log plots (normalized concentration vs. log of time). The semi-log plot is used in this study to judge the quality of a

Table 2. Results of Numerical Simulation for 1,5-NDS

		Recovery fraction, f [-]	Ave. residence time, a [h]	Peclet number Pe [-]	Discharge fraction, α [-]
MG-3D	Path 1	0.004	335	23.3	
	Path 2	0.014	1999	1.1	
	total	0.019			0.034
MG-14D	Path 1	0.002	715	141.6	
	Path 2	0.004	1498	3.0	
	total	0.005			0.014
MG-28D	Path 1	0.003	356	11.7	
	Path 2	0.001	1001	30.3	
	total	0.004			0.023
MG-30D	Path 1	0.006	663	4.6	0.007
MG-31D	Path 1	0.003	736	8.1	0.004
	TOTAL	**0.037**			

Table 3. Results of Numerical Simulation for 1,6-NDS

		Recovery fraction, f [-]	Ave. residence time, a [h]	Peclet number Pe [-]	Discharge fraction, α [-]
MG-26D	Path 1	0.0006	4894	53.2	0.0001
MG-27D	Path 1	0.0009	4897	28.1	0.0000
MG-29D	Path 1	0.0026	4668	46.1	
	Path 2	0.0002	2496	124.9	
	total	0.0028			0.0002
MG-30D	Path 1	0.0029	5591	18.1	0.0001
MG-31D	Path 1	0.0002	4000	30.0	
	Path 2	0.0006	5000	50	
	total	0.0008			0.0000
	TOTAL	**0.008**			

Table 4. Results of Numerical Simulation for 2,6-NDS

		Recovery fraction, f [-]	Ave. residence time, a [h]	Peclet number Pe [-]	Discharge fraction, α [-]
MG-7D	Path 1	0.029	2810	12.0	0.025
MG-16D	Path 1	0.064	3784	5.7	0.088
MG-2D	Path 1	0.009	2999	13.8	
	Path 2	0.011	5498	32.2	
	total	0.020			0.021
MG-22D	Path 1	0.006	3258	22.1	
	Path 2	0.008	5466	76.1	
	total	0.014			0.009
	TOTAL	**0.127**			

given data point with respect to the other data points in the same set.

Table 3 shows the results of the numerical simulation for the 1,6-NDS test. The parameter estimates indicate that Well MG-29D is most affected with a discharge fraction of 0.0002 (discharge fractions in other wells are almost zero). However, recovery fractions are very small (total of 0.008 or about 5 kg out of the original 600 kg injected). These values and the slow fluid movement indicate that the migration of the Paril groundwater that passes through Well MG-4DA has minimal impact to the production sector under the operating conditions during the test.

The Mamban fault (Fig. 1) is considered as a fluid conduit from Well MG-4DA to the production sector.

The 2,6-NDS tracer was injected at Well MG-5RD to assess the effect of hot brine and condensate injection at the MGRD1 injection sink. Results show the connection between Well MG-5RD and the wells MG-7D, MG-16D, MG-2D and MG-22D probably through the Mahanagdong fault (Fig. 1) although other conduits may exist based on the first arrival times.

The recovery profiles (Fig. 5) show fast tracer arrival in Wells MG-7D (Fig. 5(a)) and MG-16D (Fig. 5(c)) where first detection were at 20 days and 28 days, respectively. The tracer was detected in Well MG-2D (Fig. 5(b)) at day 45 and in Well MG-22D (Fig. 5(d)) at day 56. The recovery curves are almost complete for wells MG-7D and MG-16D indicating less dispersion compared to the other two wells. A single path model gives the best fit for these wells. In contrast, a two-path model is used to estimate the parameters for the incomplete recovery curves of Wells MG-2D and MG-22D. Additional data may improve the curve fitting for these wells.

Table 4 shows the results of the numerical simulation for the 1,6-NDS test. The total recovery fraction from the four wells is 0.127 or about 76 kg out of the original 600 kg of tracer injected. Highest recovery fraction is observed in Well MG-16D at 0.064 while lowest is observed in Well MG-22D at 0.014. These are equivalent to discharge fractions of 0.088 and 0.009, respectively.

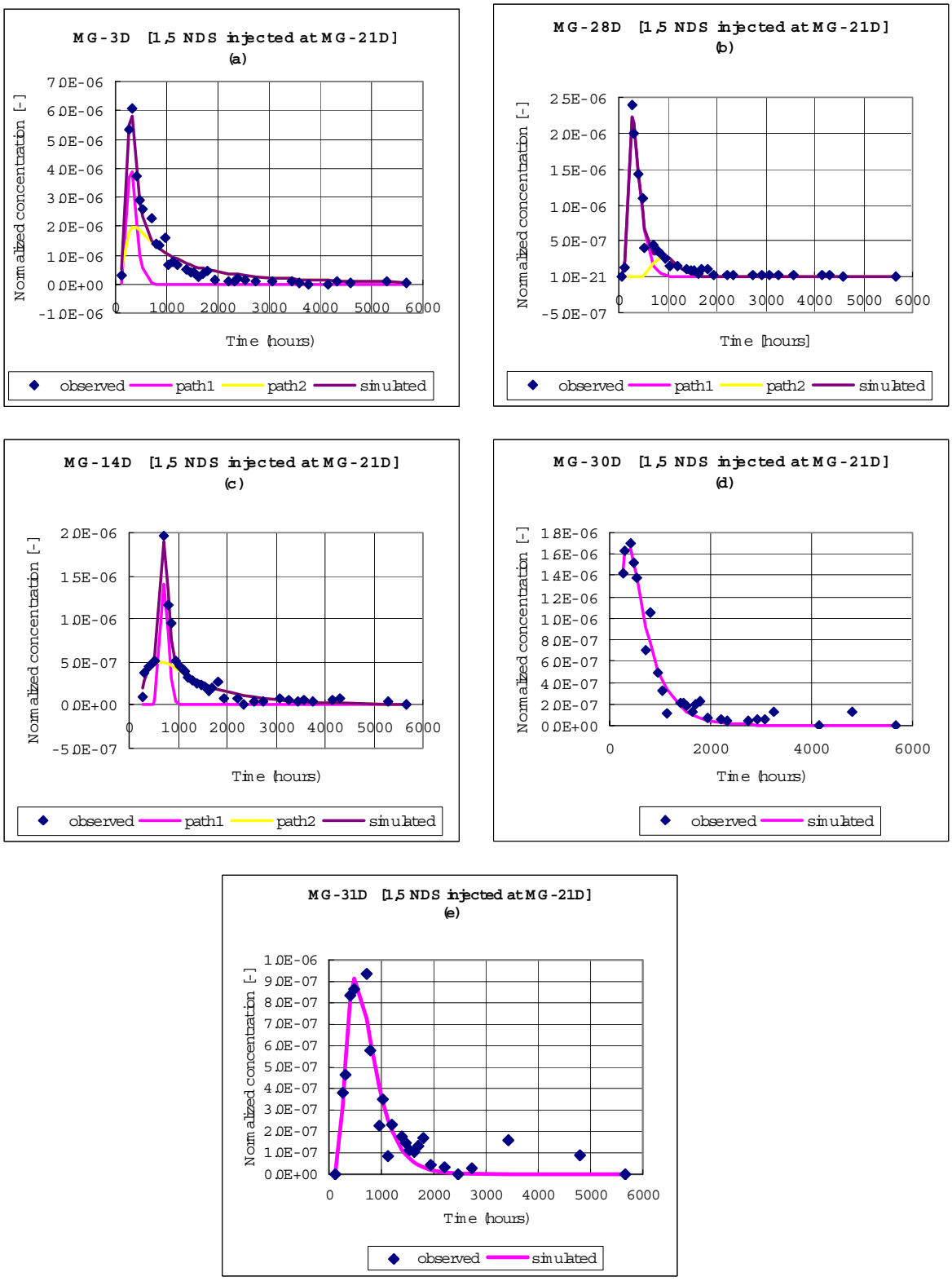

Figure 3. Results of numerical simulation for 1,5-NDS in Wells MG-3D (a), MG-28D (b), MG-14D (c), MG-30D (d) and MG-31D (e)

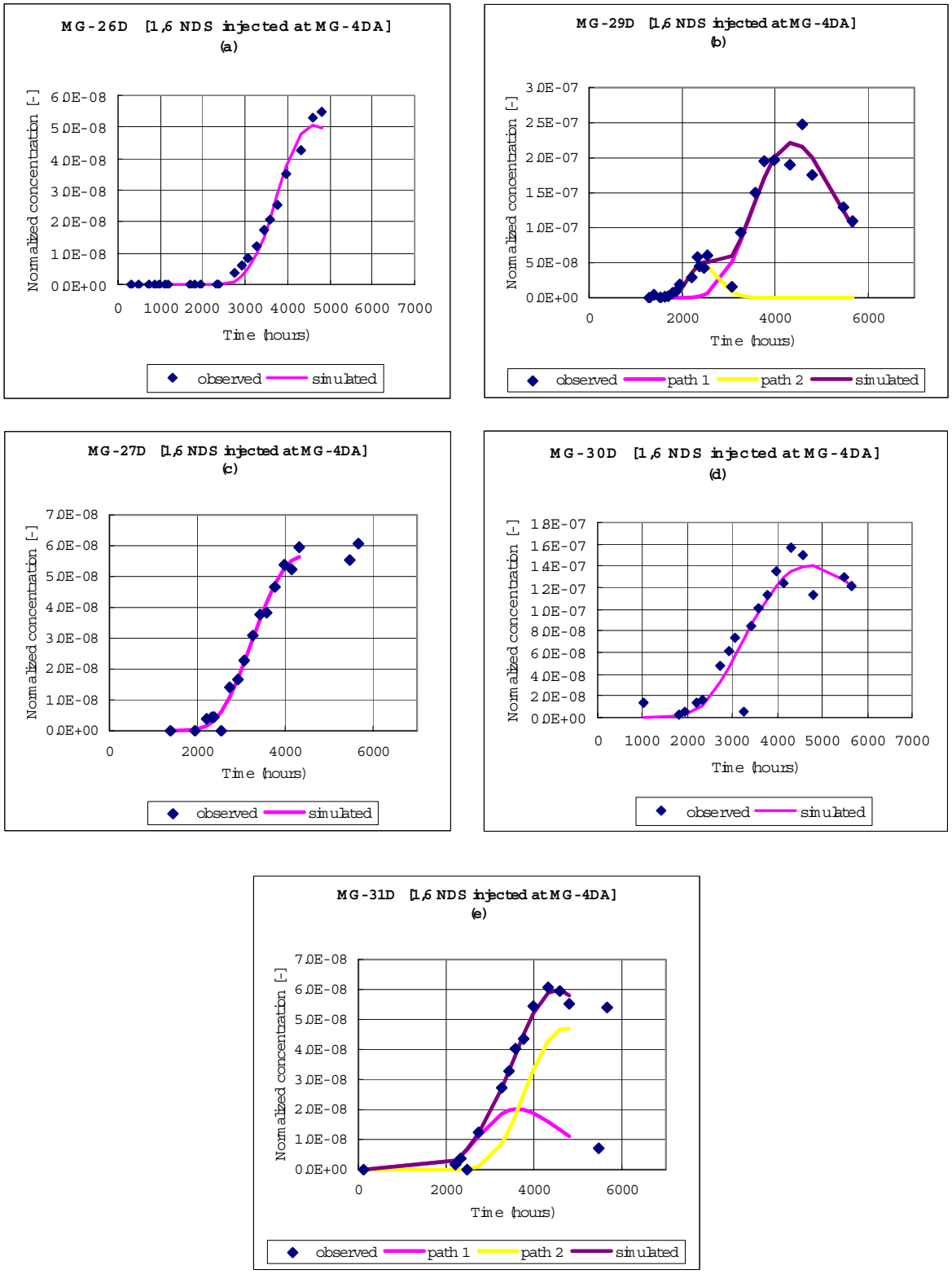

Figure 4. Results of numerical simulation for 1,6-NDS in Wells MG-26D (a), MG-29D (b), MG-27D (c), MG-30D (d) and MG-31D (e)

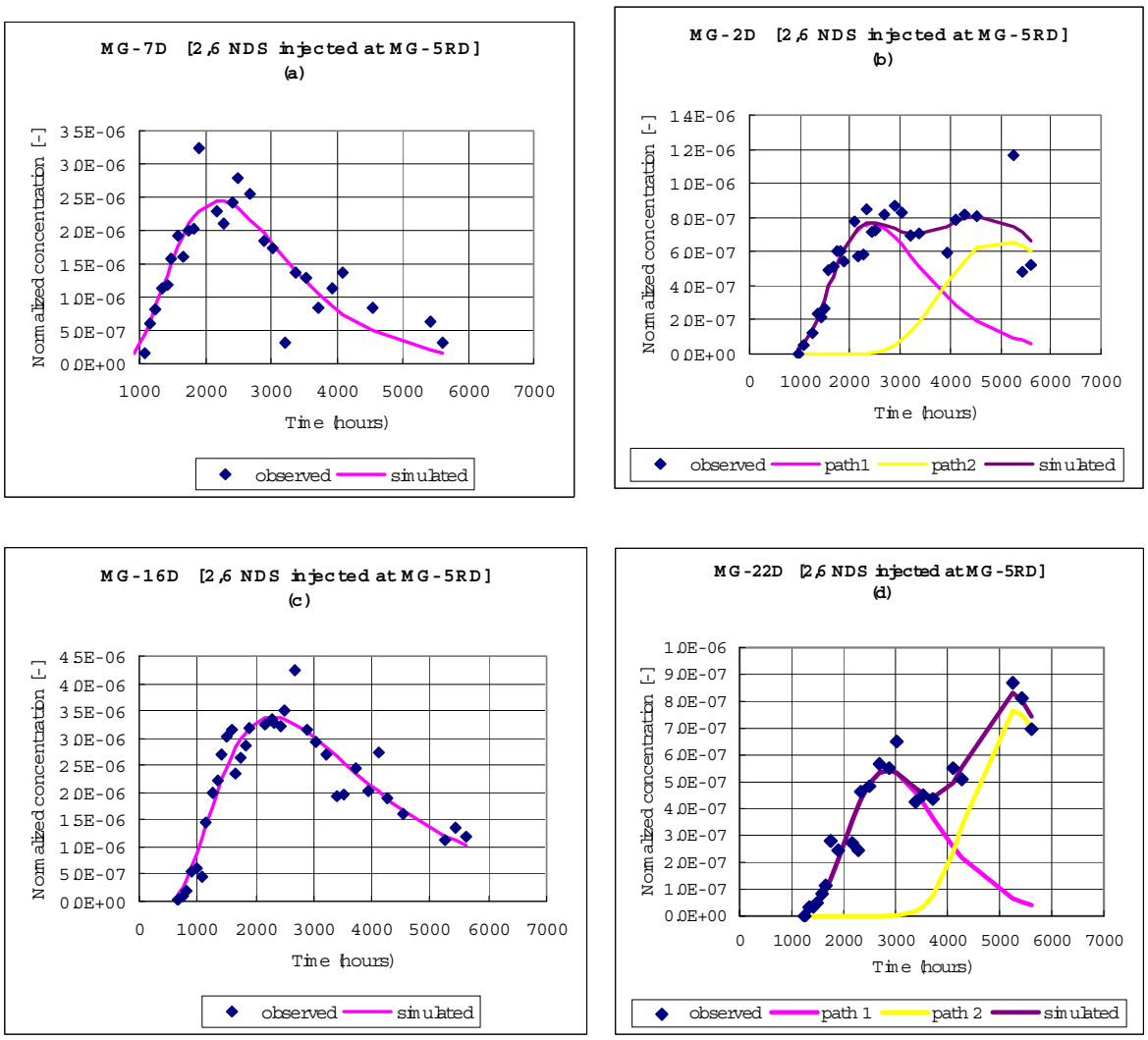

Figure 5. Results of numerical simulation for 2,6-NDS in Wells MG-7D (a), MG-2D (b), MG-16D (c) and MG-22 (d)

5. CONCLUDING REMARKS

The results of the three NDS tracer tests confirm the connection between the injection and production wells in Mahanagdong. In addition, the incursion of the Paril groundwater to the production sector through Well MG-4DA is detected. The effects of these waters are quantified in terms of recovery and discharge fractions by fitting single or two-path models to the observed data.

The fit of the curves, however, depend mainly on the quality and number of data available. A higher frequency of data at early times (Fig. 3) will give better values of the estimated parameters because there will be more data for curve fitting. High data frequency at early time ensure the detection of the first arrival and the peak concentration of the tracer. Similarly, additional data points at late time (Fig. 4 and 5) will give better results by completing the entire breakthrough curve. These additional data points will also give better semi-log plots of the curves for data quality analysis.

A wellhead to wellhead calculation of x should be avoided because this will overestimate/underestimate the values of the average fluid velocity since the wells are directional. Thus, a detailed correlation between the number of paths in the model and their physical representation (i.e., faults, permeable structures, etc.) in the reservoir and the actual location of the feed points in the wells must be studied. In this way, the actual values of x will be used to evaluate the average fluid velocity between the injection and production/observation wells.

The measured values of the groundwater temperature and flow rate inside the well will greatly improve the analysis of tracer movement from well MG-4DA. If measured values are not available, then a new model that can address this system may give better estimates of the parameters.

ACKNOWLEDGEMENTS

The data used in this study was provided by the PNOC Energy Development Corporation.

REFERENCES

Bear, J.: Hydraulics of Groundwater, McGraw-Hill : New York, 1979.

Chida, T., and Niibori, Y.: Tracer Response Analysis in a Geothermal Reservoir, *Geothermal Energy* **11** (1996), 146-157. (In Japanese)

Delfin Jr., F.G., Barry, B., Dacillo, D.B., and Marcelo, E.A.: Analysis and Interpretation of ^{125}I Tracer Test Results, Mahanagdong Geothermal Reservoir, Leyte, Philippines,

Paper presented at the IAEA RAS/8/092 and INT/0/060 Coordination Meeting on Isotopic and Geochemical Techniques in Geothermal Exploration and Reservoir Management, (2001).

Kinzelbach, W.: Groundwater Modelling, Elsevier : Amsterdam, 1986.

Kumagai, N., Tanaka, T., and Kitao, K.: Characterization of Geothermal Fluids Flow at Sumikawa Geothermal Area Using Two Types of Tracers and an Improved Multi-path Model, *Geothermics* **33** (2004), 257-275.

Rose, P.E., Johnson, S.D., and Kilbourn, P.M.: The Application of the Polyaromatic Sulfonates as Tracers in Geothermal Reservoirs, *Geothermics* **30** (2001), 617-640.

Salonga, N.D., Dacillo, D.B., and Siega, F.L.: Providing Solutions to the Rapid Changes Induced by Stressed Production in Mahanagdong geothermal field, Philippines, *Geothermics* **33** (2004), 181-212.

Sta. Ana, F.X.M., Hingoyon-Siega, C.S., and Andrino, R.P.: Mahanagdong Geothermal Sector, Greater Tongonan Field, Philippines : Reservoir Evaluation and Modeling Update, *Proceedings*, 27th Workshop on Geothermal Reservoir Engineering, Stanford University, Stanford, CA, (2002).